Superconductivity in the ternary intermetallics of $La_3Ni_4X_4$ (X = Si and Ge)

2008 J. Phys.: Condens. Matter 20 075202

(http://iopscience.iop.org/0953-8984/20/7/075202)

J. Phys.: Condens. Matter **20** (2008) 075202 (5pp) doi:10.1088/0953-8984/20/7/075202

Superconductivity in the ternary intermetallics of $La_3Ni_4X_4$ (X = Si and Ge)

H Fujii[1] **and S Kasahara**

Superconducting Materials Center, National Institute for Materials Science, 1-2-1 Sengen, Tsukuba, Ibaraki 305-0047, Japan

E-mail: fujii.hiroki@nims.go.jp

Received 17 November 2007, in final form 14 December 2007
Published 25 January 2008
Online at stacks.iop.org/JPhysCM/20/075202

Abstract

Superconductivity in the ternary intermetallics of $La_3Ni_4X_4$ (X = Si and Ge) with the combination of AlB_2 and $BaAl_4$ layers is reported. Both compounds are type II superconductors with critical temperatures (T_c) of 1.0 and 0.70 K for X = Si and Ge, respectively. The lower and the upper critical fields ($H_{c1}(0)$ and $H_{c2}(0)$) for X = Si are 107 Oe and 16.5 kOe, whereas those for X = Ge are 68 Oe and 2.6 kOe, respectively. The gradient $-dH_{c2}/dT$ of $La_3Ni_4Si_4$ is extraordinarily higher than those of the other three analogues of $La_3Ni_4Ge_4$ and $La_3Pd_4X_4$. The magnetic penetration depth ($\lambda(0)$) of 202 nm and Ginzburg–Landau coherence length ($\xi(0)$) of 14 nm are derived for X = Si, while they are 206 and 36 nm for X = Ge.

1. Introduction

Among ternary intermetallic compounds, $ThCr_2Si_2$-type intermetallics, RET_2X_2 (RE = rare earth, T = transition metal, X = Si and Ge), have been extensively studied, especially for the interest of the superconducting and magnetic properties. The structure of $ThCr_2Si_2$ is the ordered ternary derivative of the binary $BaAl_4$-type structure [1]. Although superconductivity is observed for some compounds, the critical temperature (T_c) is very low, as observed for, e.g., $LaPd_2Ge_2$ with a T_c of 1.12 K [2]. Many works were carried out for the discovery of new intermetallic superconductors with higher T_cs. Finally, quaternary intermetallic superconductors RET_2B_2C with $ThCr_2Si_2$-derivative structure showing high T_cs were discovered [3–6]. Among these compounds, YPd_2B_2C shows a T_c of 23 K, which is the highest among $ThCr_2Si_2$-type intermetallic compounds.

Apart from $ThCr_2Si_2$-type structure, another intermetallic superconductor, MgB_2, was discovered several years ago [7]. The MgB_2 shows a T_c as high as 39 K, which is the highest among intermetallic compounds. The structure of the MgB_2 is AlB_2-type structure, which is composed of alternating of hexagonal layers of Al atoms and graphite-like honeycomb layers of B atoms. Many works have been done so far on the compounds with AlB_2-type structure after the discovery of MgB_2, and several superconductors with this structure have been reported [8, 9].

We have recently reported that $La_3Pd_4X_4$ (X = Si and Ge) is type II superconductors with T_cs of 2.15 and 2.75 K for X = Si and Ge, respectively [10–13]. The crystal structure of $La_3Pd_4X_4$ is a $U_3Ni_4Si_4$-type one with the space group of $Immm$, consisting of the combination of structural units of AlB_2-type and $BaAl_4$-type layers. On the other hand, the other analog intermetallics $La_3Ni_4X_4$ (X = Si and Ge) do not show superconductivity above 1.8 K [11]. In this paper we report superconductivity in these two compounds below this temperature.

2. Experimental details

Starting materials were La (chunk, 99.9% in purity), Ni (sheet, 99.99%), Si (granule, 99.999%) and Ge (granule, 99.999%). They were arc melted with a stoichiometric ratio of $La_3Ni_4X_4$ (X = Si and Ge) under Ar gas atmosphere on a water-cooler copper hearth. The melting was repeated several times with the button turned over between each melt. The weight loss was less than 1%. After melting, the obtained buttons wrapped in a Zr foil were annealed in an evacuated silica tube at temperatures between 1173 and 1273 K for one week.

[1] Author to whom any correspondence should be addressed.

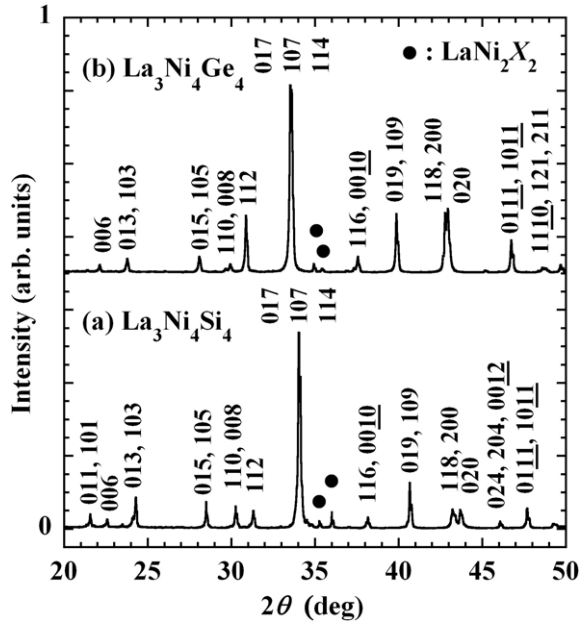

Figure 1. XRD patterns of $La_3Ni_4X_4$ (X = (a) Si and (b) Ge) samples. The indices shown in the figure are for the $La_3Ni_4X_4$ phase. The XRD peaks assigned to the corresponding $LaNi_2X_2$ phases are marked by full circles.

Samples of $LaNi_2X_2$ (X = Si and Ge) were also arc melted with a stoichiometric ratio of each material, and subsequently annealed in an evacuated silica tube at 1173 K for one week.

Phase identification was carried out for crushed samples by an x-ray diffraction (XRD) method with an x-ray diffractometer JEOL JDX-3500 with Cu K_α radiation. Microstructural observation was carried out using a scanning electron microscope (SEM) JEOL JSM-6301F with an energy dispersive x-ray (EDX) spectrometer.

Magnetization measurements were performed for polished polycrystalline samples by a micro-Hall probe technique, with a Hall probe fabricated from two-dimensional electron gas of GaAs/AlGaAs heterostructure. The active area of the Hall probe is $30\times30\ \mu m^2$ with available sensitivity of about 10 mG. Magnetic induction perpendicular to the Hall probe (B_z) is given by measuring the field-linear Hall resistance appearing across the active area. Subtracting an applied field (H_a) from the magnetic induction (B_z), the magnetization $4\pi M_l = B_z - H_a$ is obtained for a local area of the magnetic material. Field- and temperature-dependent magnetization curves were recorded at temperatures above 0.35 K in magnetic fields up to 500 Oe. The T_c was defined as the onset temperature where a diamagnetic signal was observed. The first penetration field (H_{fp}) is proportional to lower critical field (H_{c1}) [14]:

$$H_{fp}/H_{c1} = \tanh\sqrt{0.36b/a},$$

where a and b represent sample lengths perpendicular and parallel to H_a, respectively. The samples in the present experiments were prepared so as to have the dimensions of $a \approx b$, leading to the field ratio H_{fp}/H_{c1}.0.5. The $H_{fp}(T)$ was taken as the first deviation point of the $4\pi M_l(H_a)$ curves from the linear Meissner slopes observed in the low-field region.

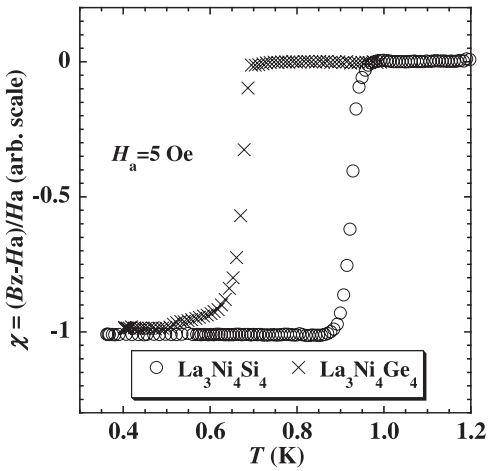

Figure 2. Temperature dependence of local magnetization curves in an applied field H_a of 5 Oe for $La_3Ni_4X_4$ (X = Si and Ge).

The magnetization is measured locally by this method, and hence, we investigated a few pieces of the samples to check reproducibility.

Electrical resistivity (ρ) measurements were carried out for a few pieces of each sample in the temperature range from 0.3 to 300 K in magnetic fields up to 11 kOe by a standard DC four-probe method. Upper critical fields (H_{c2}^{on} and H_{c2}^{off}) were estimated, taking account of 10 and 90 % decreases in ρ at superconducting transition of the $\rho(T)$ curves, respectively.

3. Results and discussion

XRD patterns of $La_3Ni_4X_4$ samples are shown in figures 1(a) and (b) for X = Si and Ge, respectively. The XRD analyses indicate that $La_3Ni_4X_4$ phases are present as a major phase with a small amount of impurity phases $LaNi_2X_2$ as reported previously [11]. The content of $LaNi_2X_2$ is estimated to be about several per cents for both samples. The lattice parameters of $La_3Ni_4X_4$ are $a = 0.413\,08(5)$ nm, $b = 0417\,60(5)$ nm and $c = 2.3578(3)$ nm for X = Si, and $a = 0.420\,17(2)$ nm, $b = 0.421\,67(3)$ nm and $c = 2.4031(1)$ nm for X = Ge. On the other hand, for $LaNi_2X_2$ samples, all the peaks in the corresponding XRD patterns are indexed on the basis of body-centered lattice with space group of $I4/mmm$, indicating that the samples are obtained as a single phase.

Figure 2 shows temperature dependence of magnetization curves in an H_a of 5 Oe for $La_3Ni_4X_4$. The T_cs are 1.0 and 0.70 K for X = Si and Ge, respectively. They are almost equal to the zero resistance temperatures, as mentioned below. Figure 3 shows magnetization hysteresis curves of $La_3Ni_4X_4$ for X = Si and Ge at 0.35 K, respectively. These hysteresis curves indicate that both compounds are type II superconductors. The initial linear Meissner slopes for both samples roughly corresponds to $-1/4\pi$, indicating the almost perfect shielding of these samples.

H_{c1} was estimated from the magnetization hysteresis curves measured at various temperatures. Figure 4 shows the $H_{c1}(T)$ curves fitted with the formula $H_{c1} = H_{c1}(0)[1 - (T/T_c)^2]$. These fittings result in $H_{c1}(0) = 107$ and 68 Oe for

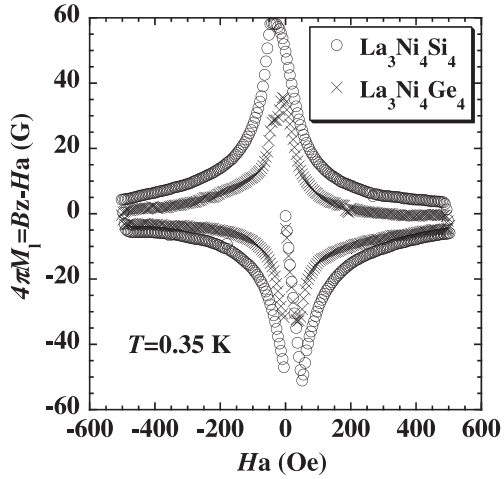

Figure 3. Magnetization hysteresis curves of $La_3Ni_4X_4$ (X = Si and Ge) measured at 0.35 K.

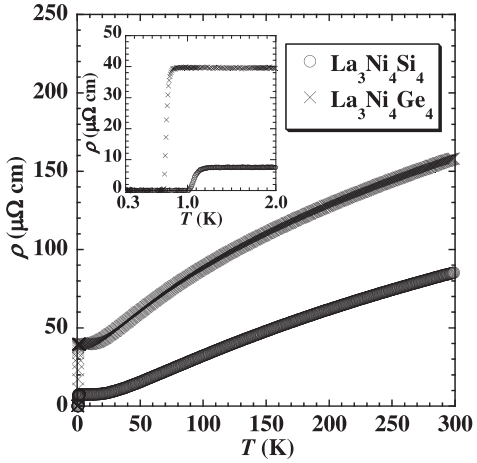

Figure 5. Temperature-dependent electrical resistivity ρ for $La_3Ni_4X_4$ (X = Si and Ge). The insets show the detail of the region in the vicinity of T_c.

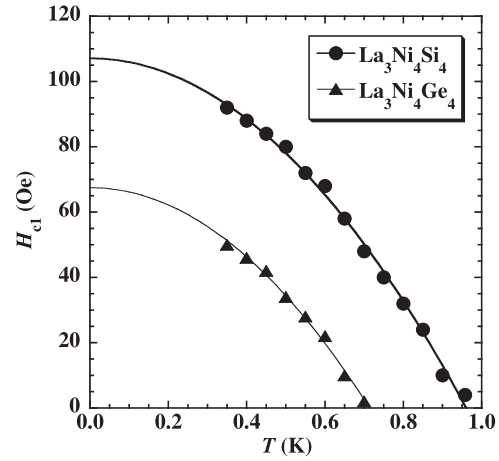

Figure 4. Lower critical field H_{c1} as a function of temperature for $La_3Ni_4X_4$ (X = Si and Ge). The H_{c1} data are fitted with the formula $H_{c1} = H_{c1}(0)[1 - (T/T_c)^2]$.

$La_3Ni_4Si_4$ and $La_3Ni_4Ge_4$, respectively. They are higher than those of the analogues $La_3Pd_4X_4$, whereas much lower than that of intermetallic Ni-based borocarbide superconductors (around 800 Oe) [15] and MgB_2 (around 400 Oe) [16].

Figure 5 shows $\rho(T)$ curves for $La_3Ni_4X_4$. Both samples show zero resistance at low temperature. The details of the region in the vicinity of T_c are shown in the inset. The resistivity decreases with decreasing temperature, showing metallic-type conductivity with a small negative curvature from 300 to 30 K for both samples. The onset temperature of the resistivity transition is 1.2 K, and zero resistance is observed at 1.0 K for $La_3Ni_4Si_4$. On the other hand, $La_3Ni_4Ge_4$ shows the onset temperature of 0.83 K and zero resistance at 0.73 K.

As mentioned above, XRD analyses indicate that the $La_3Ni_4X_4$ samples contain a small amount of the corresponding $LaNi_2X_2$ as a major impurity phase. This phase might be responsible for superconductivity in the samples of $La_3Ni_4X_4$. However, the measurements of $\rho(T)$ curves for the $LaNi_2X_2$ revealed that neither of them shows any drop of resistivity above 0.3 K. Therefore, with the almost perfect shielding of the $La_3Ni_4X_4$ samples in the magnetization measurements as mentioned above, the superconductivity observed for the $La_3Ni_4X_4$ samples is due to the corresponding $La_3Ni_4X_4$ phase.

Figures 6(a) and (b) show the $\rho(T)$ curves in various magnetic fields for $La_3Ni_4Si_4$ and $La_3Ni_4Ge_4$, respectively. Superconductivity is suppressed by applying the magnetic fields. With increasing the fields, the transition of the $\rho(T)$ curves becomes broader. This is much more appreciable and brings about the large difference between H_{c2}^{on} and H_{c2}^{off} for $La_3Ni_4Si_4$. Figure 7 shows H_{c2}^{on} and H_{c2}^{off} as a function of temperature for $La_3Ni_4X_4$. The $H_{c2}^{on}(T)$ curve of $La_3Ni_4Si_4$ shows a positive curvature in the vicinity of T_c, similar to other superconductors, such as borocarbides [15] and Li_2Pd_3B [17]. Enlargement of the $H_{c2}^{on}(T)$ curve of $La_3Ni_4Ge_4$ also reveals such a positive curvature in the vicinity of T_c. Except for this region, the gradients $-dH_{c2}^{on}/dT$ are estimated to be 17.0 and 5.3 kOe K^{-1} for X = Si and Ge, respectively. The gradient $-dH_{c2}^{on}/dT$ for $La_3Ni_4Si_4$ is much larger than that of $La_3Ni_4Ge_4$. On the other hand, the difference of the gradient $-dH_{c2}^{off}/dT$ between these compounds is smaller, and the gradients are 6.7 and 3.9 kOe K^{-1} for X = Si and Ge, respectively. Linear extrapolation of the $H_{c2}^{on}(T)$ curves gives a large $H_{c2}^{on}(0)$ value of 16.5 kOe for X = Si, whereas the extrapolation gives $H_{c2}^{on}(0) = 4.0$ kOe for X = Ge. Assuming the Werthamer–Hefland–Hohenberg (WHH) formula $H_{c2}(0)^{WHH} = -0.69T_c(dH_{c2}/dT)_{T_c}$ [18, 19], $H_{c2}(0)^{WHH}$ of 11.7 and 2.6 kOe are obtained for X = Si and Ge, respectively, using dH_{c2}^{on}/dT as dH_{c2}/dT. For $La_3Ni_4Si_4$, upturn of the $H_{c2}^{on}(T)$ curve is observed, and the corresponding $H_{c2}(0)^{WHH}$ seems far deviated from $H_{c2}^{on}(0)$ deduced from the observed $H_{c2}^{on}(T)$ curve. In the following calculations, $H_{c2}(0)$ obtained by the linear extrapolation of the $H_{c2}^{on}(T)$ curves was used for $La_3Ni_4Si_4$ to avoid an inappropriate estimation due to the largely deviated $H_{c2}(0)^{WHH}$. On the other hand, the $H_{c2}(0)^{WHH}$ value for $La_3Ni_4Ge_4$ is applicable for $H_{c2}(0)$.

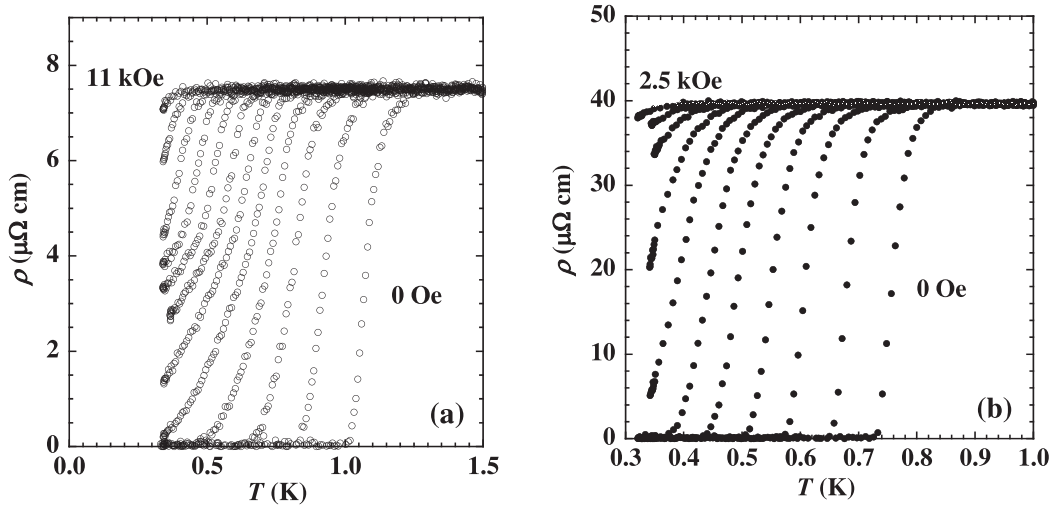

Figure 6. $\rho(T)$ curves in various magnetic fields for (a) $La_3Ni_4Si_4$ and (b) $La_3Ni_4Ge_4$. The fields were changed stepwise from 0 to 11 kOe by 1 kOe for (a), and from 0 to 2.5 kOe by 250 Oe for (b).

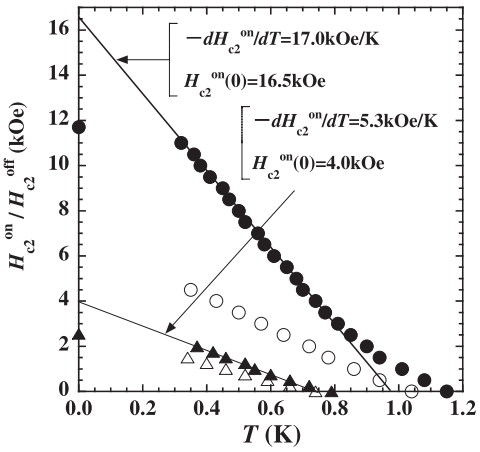

Figure 7. Upper critical fields (H_{c2}^{on} and H_{c2}^{off}) as a function of temperature for $La_3Ni_4X_4$ (X = Si and Ge). The H_{c2}^{on} and H_{c2}^{off} were estimated, taking account of 10 and 90% decrease in ρ at superconducting transition of the $\rho(T)$ curves, respectively. Solid and open circles represent H_{c2}^{on} and H_{c2}^{off} for $La_3Ni_4Si_4$, respectively, whereas the corresponding triangles represent H_{c2}^{on} and H_{c2}^{off} for $La_3Ni_4Ge_4$. The H_{c2} values at 0 K for both compounds are calculated from WHH theory using dH_{c2}^{on}/dT as dH_{c2}/dT.

With the formula $H_{c2}(0) = \Phi_0/2\pi\xi(0)^2$ (Φ_0 is the flux quantum), the Ginzburg–Landau coherence lengths $\xi(0)$ are calculated. The $\xi(0)$ are estimated to be 14 and 36 nm for X = Si and Ge, respectively. The $\xi(0)$ value of $La_3Ni_4Ge_4$ is comparable to the value of 38 nm for $La_3Pd_4Si_4$ [11] and that of 33 nm for $La_3Pd_4Ge_4$ [10]. These $\xi(0)$ values of $La_3Ni_4Ge_4$ and $La_3Pd_4X_4$ are several times larger than those of borocarbide superconductors [5, 15] and MgB_2 [16]. From $H_{c2}(0)$ and $\xi(0)$, the magnetic penetration depths $\lambda(0)$ are calculated to be 202 and 206 nm for X = Si and Ge, respectively, with the formula $H_{c1}(0) = (\Phi_0/4\pi\lambda^2)\ln(\lambda/\xi)$. These values are comparable to that of $La_3Pd_4Ge_4$ with 248 nm. The Ginzburg–Landau parameters ($\kappa(0)$) are 14.3 and 5.8 for X = Si and Ge, respectively, derived from the formula $\kappa(0) = \lambda(0)/\xi(0)$. On the other hand, thermodynamic critical fields ($H_c(0)$) are 816 and 314 Oe, with the formula of $H_c(0) = H_{c2}(0)/\sqrt{2}\kappa(0)$. Table 1 lists measured and derived superconducting parameters for $La_3M_4X_4$ (M = Ni and Pd; X = Si and Ge) [10, 11].

The high $-dH_{c2}^{on}/dT$ values are observed for $La_3Ni_4X_4$, compared with the analogues $La_3Pd_4X_4$. This is more appreciable for $La_3Ni_4Si_4$. Possible large anisotropy in $H_{c2}(0)$ originated in crystal structure with a large $c/a(b)$ ratio can bring about such enhancement, if aligned microstructure of crystals was present in the $La_3Ni_4Si_4$ samples. However, it is unlikely that such aligned microstructure was observed only for all the pieces of the $La_3Ni_4Si_4$ samples for the resistivity measurements.

On the other hand, the broad transition in the magnetic fields is observed and the enhancement of the gradient $-dH_{c2}^{off}/dT$ is less appreciable for $La_3Ni_4Si_4$, as shown in figures 6(a) and 7. This might imply the coexistence of a small amount of another La–Ni–Si superconducting phase in the $La_3Ni_4Si_4$ samples, e.g., such as LaNiSi with a T_c of 1.26 K [20]. Contribution of such a small amount of superconducting phase to the magnetization signals can be negligible. Moreover, specific heat measurements of the $La_3Ni_4Si_4$ samples revealed that the bulk T_c is 1.0 K and that no trace of other superconducting materials is present in the samples [21]. The onset critical temperature (T_c^{on}) and the thermodynamic critical temperature considering the entropy balance (T_c^{th}) estimated from the specific heat measurements are 1.00 and 0.96 K for $La_3Ni_4Si_4$, respectively. On the other hand, they are 0.76 and 0.74 K for $La_3Ni_4Ge_4$. They are in agreement with the results of the magnetization and electrical resistivity measurements. Therefore, we can conclude that $La_3Ni_4Si_4$ phase is at least a type II superconductor with a T_c of 1.0 K from figures 2 and 3. Although a very small amount of possible secondary superconducting phase can bring about a drop of resistivity, the extraordinarily high $H_{c2}(0)$, or $-dH_{c2}^{on}/dT$, observed for $La_3Ni_4Si_4$ may suggest two-gap nature of the superconductivity in this compound [22]. These possibilities of the coexistence of another superconducting phase or the two-gap nature can also bring about the large

Table 1. Measured and derived superconducting parameters for $La_3M_4X_4$ (M = Ni and Pd; X = Si and Ge) [10, 11].

	$La_3Ni_4Si_4$	$La_3Ni_4Ge_4$	$La_3Pd_4Si_4$ [11]	$La_3Pd_4Ge_4$ [10]
T_c (K)	1.0	0.70	2.15	2.75
$H_c(0)$ (Oe)	816	314	157	280
$H_{c1}(0)$ (Oe)	107	68	28	54
$H_{c2}(0)$ (kOe)	16.5[a]	2.6[b]	2.2[b]	3.0[b]
$-dH_{c2}^{on}/dT$ (kOe K^{-1})	17.0	5.3	1.5[c]	1.6[c]
$\lambda(0)$ (nm)	202	206	376	248
$\xi(0)$ (nm)	14	36	38	33
$\kappa(0)$	14.3	5.8	9.9	7.5

[a] $H_{c2}(0)$ were estimated by the linear extrapolation of the $H_{c2}^{on}(T)$ curves shown in figure 7.
[b] $H_{c2}(0)$ were estimated by the linear extrapolation of the $H_{c2}^{on}(T)$ curves from the WHH theory.
[c] The gradient $-dH_{c2}/dT$ was estimated from magnetization measurements.

difference between $H_{c1}(T)$ and $H_{c2}(T)$ in behavior for this compound. The $H_{c1}(T)$ curve of $La_3Ni_4Si_4$ shown in figure 4 is not extraordinary, compared with those of the other analogues, $La_3Ni_4Ge_4$ and $La_3Pd_4X_4$. For further discussions, studies using single crystalline samples are required.

4. Conclusion

The ternary intermetallics of $La_3Ni_4X_4$ (X = Si and Ge) with $U_3Ni_4Si_4$-type structure with the combination of structural units of AlB_2-type and $BaAl_4$-type layers are type II superconductors. The T_cs are 1.0 and 0.70 K for X = Si and Ge, respectively. They are lower than those of the analog compounds $La_3Pd_4Si_4$ (2.15 K) and $La_3Pd_4Ge_4$ (2.75 K). The $BaAl_4$ ($ThCr_2Si_2$)-type $LaNi_2X_2$, one of the layers in $La_3Ni_4X_4$, do not show superconductivity above 0.3 K for both Si and Ge. $H_{c1}(0)$ are 107 and 68 Oe for $La_3Ni_4Si_4$ and $La_3Ni_4Ge_4$, respectively. The $H_{c2}(0)$ estimated by linear extrapolation is 16.5 kOe for $La_3Ni_4Si_4$, whereas the $H_{c2}(0)$ estimated by WHH theory is 2.6 kOe for $La_3Ni_4Ge_4$. The gradient $-dH_{c2}/dT$ of $La_3Ni_4Si_4$ is extraordinarily higher than the other three analogues of $La_3Ni_4Ge_4$ and $La_3Pd_4X_4$. A very small amount of another superconducting phase with high H_{c2} which might be present in the $La_3Ni_4Si_4$ samples may contribute to superconducting transition and increase the $H_{c2}(0)$ value. Studies using single crystalline samples are awaited.

Acknowledgments

The authors cordially thank Drs Nakane, Mochiku, Takeya, Ooi and Hirata for helpful discussions. SK is supported by a Grant-in-Aid Scientific Research, Young Scientists (B), from the Ministry of Education, Culture, Sports, and Science and Technology (MEXT), Japan.

References

[1] Ban Z and Sikirica M 1965 *Acta Crystallogr.* **18** 594
[2] Hull G W, Wernick J H, Geballe T H, Waszczak J V and Bernardini J E 1981 *Phys. Rev.* B **24** 6715
[3] Cava R J, Takagi H, Batlogg B, Zandbergen H W, Krajewski J J, Peck W F Jr, van Dover R B, Felder R J, Siegrist T, Mizuhashi K, Lee J O, Eisaki H, Carter S A and Uchida S 1994 *Nature* **367** 146
[4] Cava R J, Takagi H, Zandbergen H W, Krajewski J J, Peck W F Jr, Siegrist T, Batlogg B, van Dover R B, Felder R J, Mizuhashi K, Lee J O, Eisaki H and Uchida S 1994 *Nature* **367** 252
[5] Cava R J, Batlogg B, Siegrist T, Krajewski J J, Peck W F Jr, Carter S, Felder R J, Takagi H and van Dover R B 1994 *Phys. Rev.* B **49** 12384
[6] Fujii H, Ikeda S, Kimura T, Arisawa S-i, Hirata K, Kumakura H, Kadowaki K and Togano K 1994 *Japan. J. Appl. Phys.* **33** L590
[7] Nagamatsu J, Nakagawa N, Muranaka T, Zenitani Y and Akimitsu J 2001 *Nature* **410** 63
[8] Cooper A S, Corenzwit E, Longinotti L D, Matthias B T and Zachariasen W H 1970 *Proc. Natl Acad. Sci.* **67** 313
[9] Imai M, Abe E, Ye J, Nishida K, Kimura T, Honma K, Abe H and Kitazawa H 2001 *Phys. Rev. Lett.* **87** 077003
[10] Fujii H, Mochiku T, Takeya H and Sato A 2005 *Phys. Rev.* B **72** 214520
[11] Fujii H 2006 *J. Phys.: Condens. Matter* **18** 8037
[12] Mochiku T, Fujii H, Takeya H, Wuernisha T, Mori K, Ishigaki K, Kamiyama T and Hirata K 2007 *Physica* C **463–465** 182
[13] Kasahara S, Fujii H, Mochiku T, Takeya H and Hirata K 2008 *Physica* B at press
[14] Brandt E H 1999 *Phys. Rev.* B **60** 11939
[15] Takagi H, Cava R J, Eisaki H, Lee J O, Mizuhashi K, Batlogg B, Uchida S, Krajewski J J and Peck W F Jr 1994 *Physica* C **228** 389
[16] Buzea C and Yamashita T 2001 *Supercond. Sci. Technol.* **14** R115
[17] Togano K, Badica P, Nakamori Y, Orimo S, Takeya H and Hirata K 2004 *Phys. Rev. Lett.* **93** 247004
[18] Helfand E and Werthamer W R 1966 *Phys. Rev.* **147** 288
[19] Werthamer N R, Helfand E and Hohenberg P C 1966 *Phys. Rev.* **147** 295
[20] Lee W H, Yang F A, Shih C R and Yang H D 1994 *Phys. Rev.* B **50** 6523
[21] Kasahara S, Fujii H, Mochiku T, Takeya H and Hirata K 2008 *Phys. Rev.* B submitted
[22] Gurevich A 2003 *Phys. Rev.* B **67** 184515